# Efficient Image Fusion Algorithm for Multi-Focus Images Using Energy Estimation

Yingjie Zhang[1] and Liling Ge[2]

[1]School of Mechanical Engineering, Xi'an Jiaotong University,
Xi'an, Shaanxi, People's Republic of China, 710049
yjzhang@mail.xjtu.edu.cn

[2]School of Material Engineering, Xi'an University of Technology,
Xi'an, Shaanxi, People's Republic of China, 710048
geliling-xut@163.com

**Abstract:** This paper presents a new image fusion approach for multi-focus image fusion. Considering that for the same scene, the energies of images captured on the focus and without the focuses are different, thus, fusion decision at some regions can be made based on the magnitudes of the energy. Certainly, fusion would be easily carried out once the source images have been segmented as a sequence of regions. However, the precise segmentation is usually difficult, and it is computationally expensive. To overcome the difficulties, a course mesh or cells, in this scheme, is defined in the image domain, each element corresponding to a set of pixels of the image on a rectangle window, which is approximated as regions. After that, fusion decision on the regions may be made by measuring the magnitudes of energy. Furthermore, note that the size of the regions may affect the fusion performance, particularly at the region boundaries, but it can be reduced by selecting finer mesh, and the cells may be spitted furthermore by using the marching squares algorithm to improve the fusion quality. By numeric experiments, it has been demonstrated that the proposed method could achieve similar fusion results compared with that obtained by the multi-scale decomposition-based image fusion algorithm, and with low computational cost.

**Keywords:** Image fusion, energy function, multi-focus image, marching squares.

（Received June 21, 2006 / Accepted September 4, 2006）

## 1. Introduction

Multiple sensor modalities provide data at different spatial, temporal and spectral resolutions which allow for enhanced performance in a wide range of modern military and civilian imaging applications. It is the aim of image fusion to integrate different data in order to obtain more information than can be derived from each of the single sensor data alone. A good example is the fusion of images acquired by sensors sensitive to visible/infrared (VIR) with data from active synthetic aperture radar (SAR). The information contained in VIR imagery depends on the multi-spectral reflectivity of the target illuminated by sun light. SAR image intensities depend on the characteristics of the illuminated surface target as well as on the signal itself. The fusion of these disparate data contributes to the understanding of the objects observed. In general, image fusion methods can be grouped into two classes: color related techniques and statistical or numerical methods. The first comprises the color composition of three image channels in the RGB color space as well as more sophisticated color transformations like the Intensity-Hue-Saturation (HIS) and Hue-Saturation-Value (HSV). These methods involve the transformation of a three band combination of a multi-spectral image to an intensity, hue, and saturation color space image. The intensity component of this transformation is replaced with the panchromatic (PAN) image, and a transformation back into an RGB image is performed. Unfortunately, as stated by Liu in [1] that the spectral distortion introduced by these fusion techniques is uncontrolled and not quantified. Another disadvantage of these methods is that they are limited to three band composites.

Statistical approaches are implemented based on channel statistics including correlation and filters like the PCA method [2]. The numerical methods follow arithmetic operations such as image differencing and ratios to add a channel to other image bands. A sophisticated numerical approach uses wavelets in a multi-resolution environment. Wavelet transform is a linear tool in its original from [3], but nonlinear extensions of discrete wavelet transform are possible by various methods like lifting scheme [4]. Wavelet decompression image merger methods address the limitations described above by its ability to be performed on individual bands, and a decrease in the spectral distortion. It shows a good position of a function (here this function is the image) in spatial and frequency spaces.

This paper concerns multi-focus fusion, i.e., the source images that depict the same scene but each image was acquired with a different focus length. The fusion decision is made based on the magnitudes of the energies of the regions, and to avoid the mosaic effect at boundaries of the region, the marching squares algorithm is applied to fine the joint of different regions. The rest of this paper is organized as follows.

Section 2 introduces some related works that the theory of energy function and the marching squares algorithm. Section 3 establishes the image fusion scheme, and related modules are also described, which is followed by several numeric experiment results given in Section 4 and the results are compared with those of the previous methods. Finally the conclusions are given in Section 5.

## 2. Related Work

### 2.1 Basic Theory of Energy Function

Known from the existing segmentation and denoising approaches, the energy functional approach have been given widely attention. Details regarding the interaction and close relations between these approaches can be found in [5-7]. A classical variational denoising algorithm is the total variation (TV) minimizing process of Rudin-Osher-Fatemi [8]. This algorithm seeks an equilibrium state (minimal energy) of the energy functional comprised of the TV norm of the observed image $u$ and the fidelity of this image to the noisy input image $u_0$ :

$$E_{TV} = \int_{\Omega} (|\nabla u| + \frac{1}{2}\lambda (u - u_0)^2) dx \ , \qquad (1)$$

where $\lambda$ is a scalar controlling the fidelity of the solution to the input image (inversely proportional to the measure of denoising). The TV term $|\nabla u|$ is applied to measure the blurring effect of the fused image, and the second term (fidelity term) that measure the closeness to the original image is used to estimate the variance of detail level of fused image; The term also measures the change of contrasts of the fused image after the fusion in compassion with the reference image. The energy is defined over the image domain and typically processes local minima at the intensity edges occurring at object boundaries. Therefore the magnitude of the energy reflects the edge intensity distributions. Thus, images with more information or details will have a high energy, and images with few details will have a low energy. Due to blurring existed on the out-of-focus images, both the TV term and the fidelity term obtained from the out-of-focus image in (1) have smaller values than those from the image on the focus. It is special true for the corresponding regions from different images.

### 2.2 Marching Squares Algorithm

Marching cubes (MC) algorithm was proposed by Lorensen and Cline in [9]. It analyzes the binary pattern of eight vertices of a cube to construct a surface that approximates the underlying surface. Considering rotations and symmetries, they reduce the original 256 patterns to a total of 15 configurations. Although the marching cubes algorithm has been proved effective, it has several problems and many variants were hence proposed to address these problems.

The marching squares algorithm aims at drawing lines between interpolated values along the edges of a square, considering given weights of the corners and a reference value. The marching squares algorithm is of the “divide and conquer” type, dividing the 2-dimensional data set into a matrix of cells or squares. After the data set has been divided each square is taken individually. The basic principle behind the marching squares algorithm is that it takes each square, works out the values for the given vertices, stores them then moves onto the next. Only when all the squares within the matrix have been dealt with, can the data be presented in its entirety. There are a finite number of ways that a contour can pass through a cell. Each of these different ways is called a state. It has been proved that for any square there are only 16 ways , as shown in Fig. 1, that a contour van pass through it, these are the cases that the marching squares deals with. Each square has 4 vertices which are either inside or outside the contour this is how the state is established These 16 cases make up the lookup table for the algorithm.

To draw the curve whose value is constant and equals the reference one, different kinds of interpolation can be used. The most used is the linear interpolation, and an essential part of the algorithm is the examination of each cells vertices. There are scalar values at a finite set of points in the dataset - the cell boundaries. These points must be connected to contours. An index into the case table can be calculated by encoding the state of each vertex with a binary digit. Once the correct case has been established, then interpolation techniques can be used to work out the exact point of intersection.

In simplistic terms the algorithm can be broken down into the follows:

**Step 1.** Select a cell starting at the top left of the data-set.

**Step 2.** Calculate the inside out side state of each vertex within the cell.

**Step 3**. Calculate the vertex.

**Step 4.** Look up the topological state using the case table.

**Step 5.** Interpolate the contour value to get an exact point where the square is sliced.

**Step 6.** Move to the next cell.

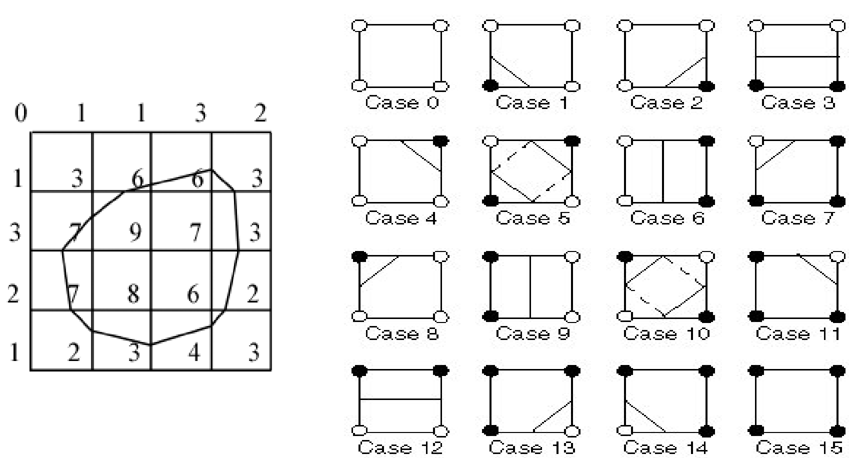


Figure 1: Lookup table for marching squares

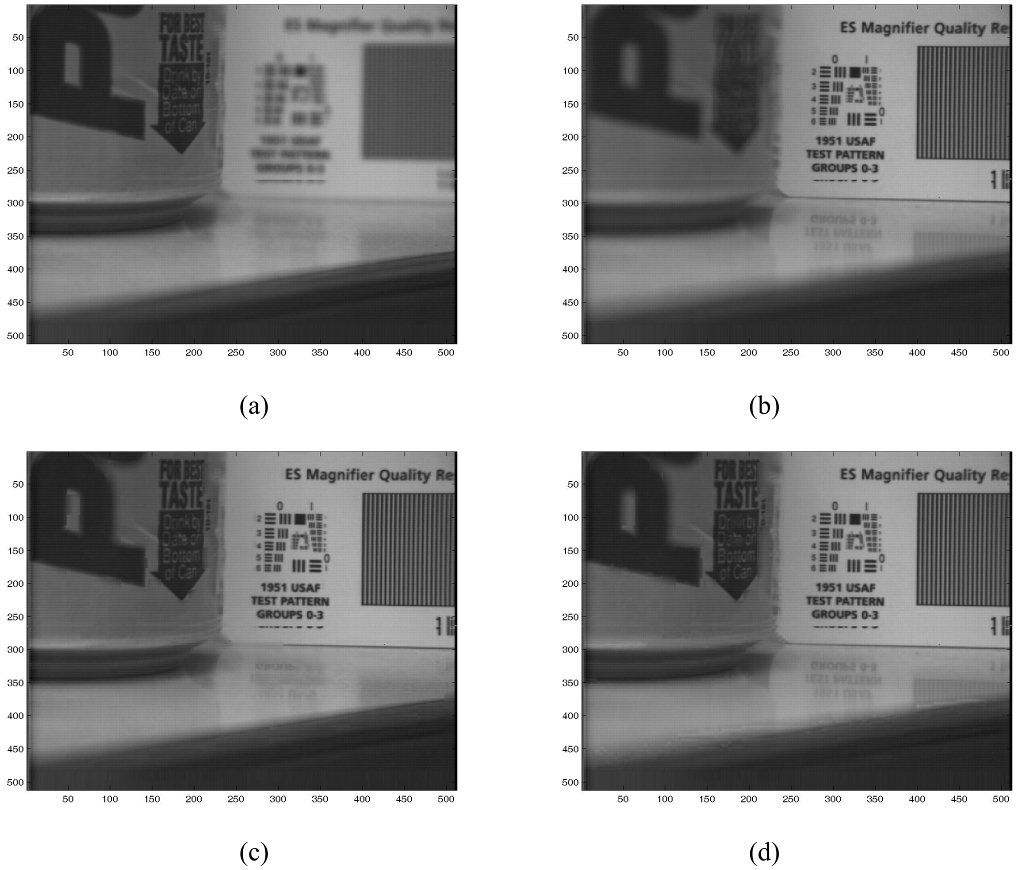


Figure 2: Comparison of fusion performances: input images in (a) and (b); results without correcting in (c) and with correcting in (d)

In this paper, the iso-value is defined by the energy values of the grid points, and only boundary points, i.e. two neighbor points or cells are from different source images respectively, are processed. The points of intersection are used to regenerate the shape of the cells of the boundary. Consequently, in the resulting fusion maps, the shapes of boundary cells will not keep as rectangle, smaller cells may be generated to improve the fusion performance. As shown in Fig 2, where (a) and (b) are the source images, and (c) and (d) represent the results obtained by the proposed method without using correcting method and with correcting by using the marching squares algorithm respectively.

## 3. Proposed Fusion Scheme

As have been pointed out previously, the image regions with and without focuses are with different energies. One may divide the image domains into a sequence of cells, then the energies for every cell in the source images are computed and compared, the cell with highest energy is selected to add into fusion maps. By this way, the fusion quality and speed completely depend on the size of cell. The larger the size of the cell is, the faster the speed of the algorithm would be. However, since the energy could not be estimated very precisely when size of cell become very small or close to the size of a pixel, as a result, some wrong composite may be resulted in for some cells, and it is computationally expensive. To solve this difficulty, consider that either the regions on the focus or the region without the focuses is continuous. Thus the cells with wrong composite can be corrected by checking the fusion decision of their neighbor cells. On the other hand, the mosaic effect generated around the region boundary could be further removed or reduced by using the marching squares algorithm to fine the boundary cells. The marching squares algorithm, in this scheme, is used to regenerate the shapes and sizes of cells for the boundary cells. The process is illustrated in Figure 3 for the case of two input images.

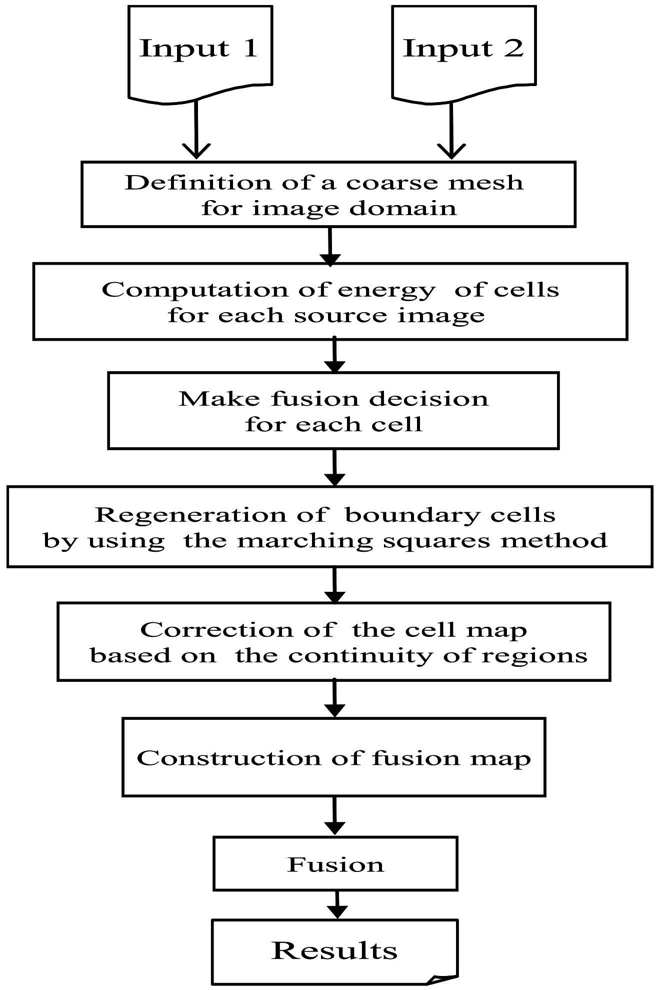


Figure 3: Block diagram of the image fusion approach

In this framework, the combination algorithm consists of six modules: the definition of a coarse mesh at image domain and computation of energy for each cell over the source images, which is then compared and selected to create the cell map that consists of 1 and 0, which represents where the cell information comes from, where 1 denotes the cell information obtained from a image and 0 denotes from another image; the boundary cells need to be further processed by the marching squares method described in section 2.2. After that, the cell map is corrected based on the continuity of the region, that is, all points either in the region with the focuses or the region without the focus have the same properties such as 1 or 0. Some discontinuity within the region can be removed and filled with the value of its neighbor points. Finally the fusion map may be created by using the cell map.

## 4. Results and Comparisons

The proposed approach has been implemented in Matlab6.5 on Microsoft WindowsXP environment and tested on a number of images, and the results are compared with previous methods in [10-13]. For simplicity, in the numeric experiments, the cell size is set as $m_x = m_y = m$, i.e., the element in the coarse mesh corresponds to a square at the image domains. The key enable technique in the algorithm is the energy model, and the energy has to be calculated for each cell. Generally speaking, the larger the size of the cell is, the more precise the energy estimation would be obtained. Therefore, the size of the region should be selected big enough so that the good energy estimation could be obtained. By numerical experiment the best region size should be bigger than 8×8.

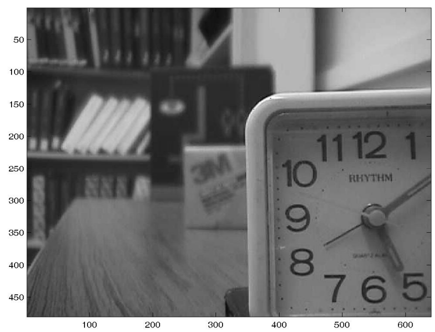


(a) Input image A


(b) Input image B

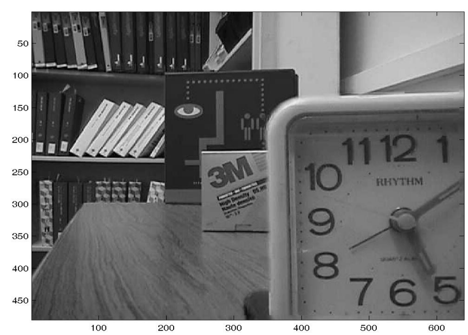


(c) The fused image obtained by the proposed method

Figure 4: Fusion of multi-focus office images

Fig. 4 shows two multi-focus office images, where the cell size $m_x$ and $m_y$ are assigned as 16 and the weighting parameter $\lambda$=0.028 for computation of the energy function. The source images are shown in (a) and (b), respectively, and the fused image in (c). Fig. 5 shows three multi-focus images to be fused. Other parameters such as the size of the cell and the weighting parameter $\lambda$ are the same with those in Figure 4. The source images are shown in (a), (b) and (c), and the resulting image is shown in (d).

To demonstrate our numerical results, for the images in Fig. 4 and Figure 5, the proposed method is compared to various multi-resolution decompositions and fusion schemes, like the pixel-based averaging method, Principal Component Analysis method (PCA), etc. Several evaluation methods, for example the root mean square error (RMSE) which is used as the evaluation criterion between the reference image and the fused image, standard deviation (SD), which is the square root of the variance, reflects the spread in the data, the entropy which is used as a measure of information content that is the average number of nits needed to quantize the intensities in the image, the cross entropy that evaluates the information difference between the two images to give the grey distribution of them, and the correlation (CORR) between the fused image and the original image, and the magnitudes of energy among the fused images also are calculated and compared. The results are exhibited in Table 1. It is clear that the proposed method outperformed the others.

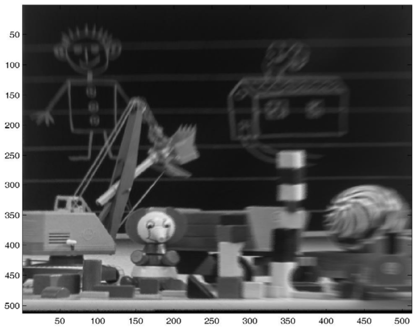

(a) Input image A

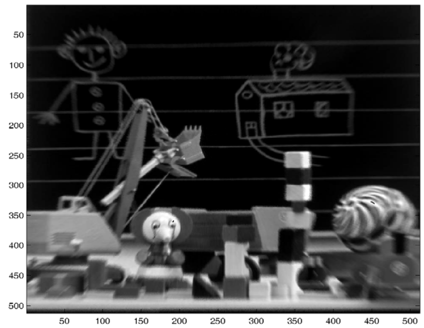

(b) Input image B

(c) Input image C

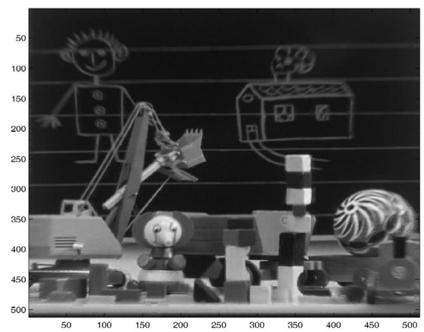

(d) Result obtained by the proposed method

Figure 5: Fusion of multi-focus office images

Table 1: Comparison of the results by using several evaluation methods

| | Methods | Entropy | Cross Entropy | CORR | SD | RMSE | Energy |
|---|---|---|---|---|---|---|---|
| **Fig.4** | **Average** | 4.7822 | 1.2894 | 0.7906 | 33.3076 | 25.7100 | 0.3581 |
| | **PCA** | 4.5917 | 2.3752 | 0.8067 | 65.1407 | 35.2116 | 0.3832 |
| | **Max** | 3.9715 | 0.7345 | 0.7919 | 56.1162 | 33.4767 | 0.3904 |
| | **Min** | 1.5185 | -0.0646 | 0.3278 | 14.9178 | 39.1286 | 0.1378 |
| | **Proposed** | 4.4995 | 2.2482 | 0.8087 | 65.4615 | 35.5667 | 0.4812 |
| **Fig.5** | **Average** | 7.1828 | 0.1458 | 0.9964 | 107.8074 | 9.1439 | 0.3081 |
| | **PCA** | 7.1849 | 0.1347 | 0.9961 | 107.6955 | 9.4462 | 0.3112 |
| | **Max** | 7.1475 | 0.0712 | 0.9935 | 112.7557 | 12.5125 | 0.2947 |
| | **Min** | 7.1293 | 0.0707 | 0.9920 | 103.5971 | 13.3671 | 0.3044 |
| | **Proposed** | 7.2450 | 0.1837 | 0.9889 | 113.3761 | 16.4087 | 0.3103 |

## 5. Conclusions

On basis of some characteristics of multi-focus images such as the continuity of regions and the regions on the focus with high energy, this paper presents a simple and efficient image fusion scheme. In comparison with previous methods, the source images are divided into a sequence of cells, and the energy for each cell is computed over the source images, consequently the cell information is obtained from the image with highest energy at the corresponding cell. To solve the mosaic effect at the boundary, the marching squares algorithm is used on the cell map to modify the shape of the boundary cells so that fusion quality can be improved further. By the number of numeric experiments, it has been demonstrated that the proposed method achieves similar fusion results. However, since the TV term in ROF model may not be estimated precisely when the small size of cell is selected, therefore, the weighting parameter $\lambda$ in ROF model has to be given carefully for the good fusion quality. How to estimate the cell energy precisely still needs to be researched further.

**Acknowledgements**

This work was supported in part by National Hi-Tech Research and Development Program of China (863 program) under Grant No.2006AA04Z142 and Shaanxi Province Science Foundation under Grant No.2006K05-G22.

**References**

[1] Liu, J. G. Smoothing filter-based modulation: a spectral preserve image fusion technique for improving spatial details, International Journal of Remote Sensing, v. 21(18), p. 3461-3472, 2000.

[2] Mouat, D. A., Mahin, G. G. and Lancaster, J. Remote sensing techniques in the analysis of change detection, Geocarto International, v. 2, p. 39- 50, 1993.

[3] Mallat, S. A wavelet tour of signal processing, Academic Press, London, 1998.

[4] Claypoole, R. L., Davis, G. M. and Baraniuk, R. G. Nonlinear wavelet transforms for image coding via lifting, IEEE Transactions on Image Processing v. 12 (2), p. 1449-1459, 2006.

[5] Petrovic, V. S. and Xydeas, C. S. Sensor noise effects on signal-level image fusion performance, Information Fusion, v. 4, p. 167–183, 2003.

[6] Weickert, J. A review of nonlinear diffusion filtering, Scale-Space Theory in Computer Vision, LNCS 1252, Springer, Berlin, p. 3-28, 1997.

[7] You, Y. and Xu, W. A. Tannenbaum, M. Kaveh, Behavioral analysis of anisotropic diffusion in image processing, IEEE Trans. Image Process, v. 5(11), p. 1539-1553, 1996.

[8] Rudin, L., Osher, S., and Fatemi, E. Nonlinear total variation based noise removal algorithms, Physica, v. 60, p. 259-268, 1992.

[9] Lorensenw, E. and Cline, H. E. Marching cubes: A high resolution 3d surface construction algorithm, Proc. of ACM SIGGRAPH, p. 163-169, 1987.

[10] Zhang, Z. and Blum, R. Region-based image fusion scheme for concealed weapon detection, Proceedings of the 31st Annual Conference on Information Sciences and Systems, p. 168-173, 1997.

[11] Piella, G. A region-based multiresolution image fusion algorthim, ISIF Fusion conference, Annapolis, USA, p. 1557–1564, 2002.

[12] Lewis, J. J., O'Callaghan, R. J., Nikolov, S. G., Bull, D. R., and C. N. Canagarajah, Region-based image fusion using complex wavelets, 7th International Conference on Information Fusion, Stockholm, Sweden, 28 June International Society of Information Fusion (ISIF), p. 555-562, 2004.

[13] Mukhopadhyay, S. and Chanda, B. Fusion of 2D gray scale images using multi-scale morphology, Pattern Recognition, v. 34, p. 1939–1949, 2001.